Flexural isostatic response of the Alps to increased Quaternary erosion recorded by foreland basin remnants, SE France

Jean-Daniel Champagnac, Pieter Van Der Beek, Gaël Diraison, Samuel Dauphin

Flexural isostatic response of the Alps to increased Quaternary erosion recorded by foreland basin remnants, SE France

Jean-Daniel Champagnac[1*], Peter van der Beek[2], Gaël Diraison[2], and Samuel Dauphin[2]

1. Intitute for Mineralogy, Leibniz University, Hannover, Germany.

2. Laboratoire de Géodynamique des Chaînes Alpines, Université Joseph Fourier, Grenoble, France.

* Corresponding author:

Champagnac, Jean-Daniel

Institute of Mineralogy

University of Hannover

Callinstrasse 3

D-30167 Hannover, Germany

Email: champagnac@gmail.com

phone: +49 511 762-2222

Fax : +49 511 762-3045

Short title: W-Alpine flexural rebound due to Quaternary erosion

Submitted to Terra Nova October 14, 2007, Manuscript #TER-2007-0106

Revised version: February 1, 2008.

Abstract

We test the hypothesis that flexural isostatic compensation of the mass removed by enhanced Quaternary erosion is responsible for uplift of the Western European Alps and their forelands. We use two well-preserved and well-dated (1.8 Ma) abandonment surfaces of foreland basin remnants in SE France (the Chambaran and Valensole plateaux) as passive benchmarks for tilting of the foreland. Estimating their initial slope from morphometric scaling relationships, we determine bulk post-depositional tilting of 0.5-0.8 % for these surfaces. The calculated isostatic response of the Alpine lithosphere to erosional unloading, using the method recently proposed by Champagnac *et al.* (2007), yields a predicted tilting of 0.3-0.4 % in the considered areas, explaining approximately half of the determined post-depositional tilting. Such long-term deformation being insensitive to cyclic loading/unloading due to glaciations, we suspect the other half to be related to as yet undetermined long-wavelength and long-lived tectonic process(es).

Keywords: Isostatic rebound, Quaternary erosion, Western Alps, flexure, foreland.

1. Introduction

The relative importance of tectonic and climatic controls on the evolution of mountain belts remains a major question in geodynamics. In particular, the concept that climate change may lead to mountain peak uplift through erosional relief production and isostatic compensation remains controversial (Molnar and England, 1990, Small and Anderson, 1998, Whipple *et al.*, 1999). In the western Alps, several recent studies concur to a paradox: whereas geodetic, geologic and seismologic data demonstrate active extension within the orogen core from Miocene times onward (Sue *et al.*, 1999, Delacou *et al.*, 2004, Selverstone, 2005, Champagnac *et al.*, 2006), levelling studies attest to ongoing rock uplift within most parts of the belt (e.g., Kahle *et al.*, 1997). Deep-seated geodynamic processes such as slab break-off (Lippitsch *et al.*, 2003, Kuhlemann, 2007), de-eclogitisation of the lower crust (Kuhlemann *et al.*, 2002) or asthenospheric upwelling (Lyon-Caen and Molnar, 1989) have been proposed to explain this paradox. However, climate-related processes have also been proposed, such as post-glacial rebound (Gudmundsson, 1994), shrinking of little ice-age glaciers (Barletta *et al.*, 2006) or the isostatic response to enhanced erosion (Schlunegger and Hinderer, 2001, Cederbom *et al.*, 2004, Champagnac *et al.*, 2007).

Here we test the effect of the latter process, as predicted by recent numerical models (Champagnac *et al.*, 2007). Because of the finite flexural rigidity of the lithosphere, the area affected by isostaticaly-driven rock uplift is wider than the area affected by erosion. In the case of the western Alps, the occurrence of two well-exposed Pliocene basin remnants with preserved abandonment surfaces provides exceptional natural benchmarks to test our hypothesis and constrain the overall rebound of the belt associated with increased Quaternary erosion rates. We quantify the present-day slope of the plateau surfaces by fitting inclined planes to the surface remnants. We then use morphometric relationships to estimate the initial depositional slopes for these features. The difference between initial and present-day slope can be attributed to Quaternary tilting, the magnitude of which is compared to predictions of the numerical model.

2. The western Alps and their foreland

The high elevation and relief of the western Alps are traditionally interpreted as an effect of both recent tectonic activity and relief production during Quaternary glacial / interglacial climate cycles. Peri-alpine basins record a dramatic increase in sediment supply since ~5 Ma (Guillaume and Guillaume, 1982, Kuhlemann *et al.*, 2002), from which a near tripling of erosion rates in the western Alps can be deduced. This major change in sedimentation rates has been observed worldwide (Hay *et al.*, 1988, Zhang *et al.*, 2001) and could be related to climatic changes around this time (Molnar, 2004).

A recent study (Champagnac *et al.*, 2007) has suggested that approximately half of the present-day rock uplift observed in the Swiss Alps could result from isostatic response to increased Quaternary erosion. However, the comparison of modelled rock uplift over the last 1 Ma with present-day uplift rates is not straightforward and the lack of large-scale records of rock uplift prevents a direct comparison between data and model predictions. The presence in the western alpine foreland of two Pliocene basin remnants with well-preserved upper surfaces and an extensive river-terrace record allows testing and quantifying the hypothesis of erosion-driven rock uplift and tilting of peri-alpine areas.

The Chambaran and Valensole plateaux are the westernmost fragments of the foreland basin bordering the Alpine collision zone (e.g., Burkhard and Sommaruga, 1998, Ford *et al.*, 1999). Initial marine deposition in the western Alps foreland basin started during the Late Burdigalian and onlapped the basin floor westward during Langhian and Serravalian times (Demarcq, 1970, Clauzon, 1990, Rubino *et al.*, 1990). The basin became overfilled and fluvial deposits prograded from east to west during the Tortonian. The Messinian sea-level drop was communicated up the Rhone River by a retreating knickpoint and led to abandonment of the fluvial depositional surface and the incision of deep canyons, subsequently filled by marine ria deposits during Early Pliocene sea level rise (Clauzon, 1990, Clauzon and Rubino, 1995, Clauzon, 1996). Upon the infilling of these rias, a second (Pliocene) piedmont surface was built by fluvial progradation from the east. Final abandonment of the plateau surfaces, incision of the present-day drainage and formation of river terraces started around the Pliocene-Quaternary boundary. These remarkably flat inclined plateau surfaces currently lie 150-400 m above the major active river valleys.

2.1 The Chambaran Plateau

The Chambaran Plateau (Figure 2) is a grossly triangular-shaped plateau with an area of ~3000 km^2. Morphologically, it is made up of two surface remnants separated by the glacial Bièvre-Valloire trough

(Mandier, 1988). The plateau surface rises from 257 m a.s.l. in the southwest to 784 m a.s.l. at its eastern apex, whereas fluvial base-level at the confluence between the Rhone and Isère Rivers lies at 110 m a.s.l. The late Pliocene piedmont deposits of the plateau consist of coarse conglomerates with quarzite and strongly weathered crystalline rock pebbles embedded within a sandy clay matrix (Perriaux *et al.*, 1984, Clauzon, 1990). Extensive pebble imbrication studies indicate flow directions both from SE to NW and from NE to SW, implying that both the Rhone and Isère River catchments were a major source for the Pliocene conglomerates (Mortaz-Djalili and Perriaux, 1979, Perriaux *et al.*, 1984). Mammal remains encountered on top of the Chambaran Plateau surface date its abandonment as "Villafranchian" (i.e., Latest Pliocene-Early Quaternary; Ballesio, 1972). Quaternary incision of the Isère River is marked by a flight of fluvial terrace remnants, which are tentatively correlated to the major glacial-interglacial cycles (Bonnet and Bornand, 1970, Mandier, 1988).

2.2 The Valensole Plateau

The Valensole Plateau (Figure 3) is significantly smaller than the Chambaran Plateau (~1000 km^2), but its surface has been better preserved. The plateau has developed west of the Digne fold-and-thrust belt, which has remained active up to Quaternary times (Lickorish and Ford, 1998, Hippolyte and Dumont, 2000). The plateau surface rises from 500 m a.s.l. in the southwest to 750 m a.s.l. in the northeast, whereas the modern Bléône/Durance River valley descends from 330 m to 220 m along the plateau. The Asse River cuts the plateau into northern and southern sub-regions, the southern one being about twice as large as the northern. The eastern margin of the plateau is locally overthrust by the Digne thrust sheet, and an active fold may be present below the northern sub-plateau (Hippolyte and Dumont, 2000).

The Plio-Pleistocene sequence consists of fluvial conglomerates with local lacustrine deposits, and is locally capped by a proximal breccia along the Digne thrust front (Dubar, 1984a). Pebble lithologies and fluvial transport directions indicate local sourcing by the Asse and Verdon rivers for the eastern part of the plateau, and sediment supply by the Durance River in the western part (Gigot, 1982). The Pleistocene deposits have been dated by mammal biostratigraphy and magnetostratigraphy (Dubar *et al.*, 1998) and provide a well-constrained date for abandonment of the plateau surface at 1.8 Ma. Subsequent incision of the Durance River is recorded by a well-developed set of fluvial terraces, the long profiles of which display a characteristic fan shape, with older terraces displaying increasingly higher slopes (Dubar, 1984b; cf. Figure 3b).

3. Evidence for tilting of plateau surfaces

Quantifying post-depositional tilt for the Chambaran and Valensole plateaux requires measuring their present-day slope and estimating the depositional slopes. The present-day slopes of both plateau surfaces were determined by 3D digitization of the Pleistocene abandonment surface from geological maps projected onto a Digital Elevation Model. An inclined plane was subsequently fit to the data points (Table 1). We fitted a single plane to the Chambaran Plateau but analyzed four plateau remnants separately for Valensole. The two northern remnants are fit by south-dipping planes with relatively large slopes; systematic structure in the residuals suggests that the surfaces are not planar but may be deformed by low-amplitude (~20 m) folds with wavelength ~8 km, as previously suggested by Hippolyte and Dumont (2000). We therefore exclude the northern plateau from our further analysis. Both the Chambaran and southern Valensole plateaux are characterized by W to SW-ward dipping slopes of ~0.9% (Table 1).

The sedimentology of the uppermost conglomerates indicates that they were deposited by braided streams on large alluvial fan or piedmont surfaces sloping in the direction of fluvial transport. We use scaling laws between fan area, drainage basin area and fan slope (e.g., Hooke, 1968, Blair and McPherson, 1994, Guzzetti *et al.*, 1997, Allen and Hovius, 1998, Leeder, 1999) to estimate initial depositional slopes of the Chambaran and Valensole plateaux. Figure 4 shows area and slope data for the plateaux compared to data compilations for both small- (Crosta and Frattini, 2004) and intermediate-scale (Guzzetti *et al.*, 1997) active alluvial fans from the Alps. In order to estimate drainage areas for the source regions that contributed material to the Chambaran and Valensole plateaux respectively, we use the present-day drainage areas of the main rivers in the region. For Valensole, the combined drainage area of the Asse and Verdon rivers is 2600 km^2, consistent with the ~400 km^2 part of the plateau that was fed by these rivers as indicated by the sedimentology. For the Chambaran Plateau, the combined drainage areas of the Rhone (14000 km^2) and Isère Rivers (9450 km^2) also consistently scales with the plateau area (Figure 4a).

The present-day slopes of both the Valensole and Chambaran plateaux fall significantly above the slope-area scaling shown by present-day fans (Figure 4b). Some of the largest fans from the Guzetti *et al.* (1997) database have slopes of 0.3-0.5°, close to that of the Valensole Plateau. However, these fans are intersected by seismically active thrusts with recent surface offsets (Sileo *et al.*, 2007), and have possibly been influenced by these.

Our estimates of initial fan slopes are limited by the scatter in power-law scaling because of differences in climate, lithology, hydrodynamics and depositional process (Leeder, 1999, Dade and Verdeyen, 2007). In particular, recent numerical modelling of fan development suggests that fan slope is inversely related to precipitation (Densmore *et al.*, 2007). However, this relationship has as yet not been quantitatively established in natural datasets. Moreover, palynological data suggest that the Pliocene climate of southeastern France was, if anything, warmer and wetter than the present-day (Fauquette *et al.*, 1999, Suc and Popescu, 2005). Thus, we feel that the present-day alpine fan data provide the most relevant baseline against which to compare the present-day slopes of the plateaux.

A power-law fit to the combined data of Crosta and Frattini (2004) and Guzetti *et al.* (1997), provides best estimates of initial slopes of 0.37±0.12 % for Valensole and 0.13±0.05 % for Chambaran. The present-day slopes of the Durance and Isère Rivers are 0.35% and 0.10% respectively, consistent with the deduced paleoslopes of the plateaux. The present-day tilt of the surfaces thus appears to require ~0.5% - 0.8% of post-depositional tilting.

4. Numerical modelling of erosion-induced alpine isostasy

Champagnac *et al.* (2007) presented a numerical model of the isostatic response to Quaternary erosion of the Alps, based on the relation between mean Geophysical Relief (GR; Small and Anderson, 1998) and the sediment budget of peri-alpine basins (Kuhlemann, 2000). The GR is the difference between a surface connecting the highest points within a specified search radius and the actual topography. The GR can be viewed as a "missing volume", and increases in a log-linear manner with the size of the calculation window. The latter can thus be tuned so that the integrated GR over the study area, to which erosion of the peaks at a constant rate is added, fits the deposited sediment volume within a given time interval (see Champagnac *et al.*, 2007 for details on the method used). For this study, we used 2 Ma as the reference time span, implying a circular sliding window of 6 km radius, and then multiplied the results by 0.9 considering the abandonment age of the surfaces (1.8 Ma). The method predicts the distribution of erosion within the mountain belt, implicitly assuming relief increase by valley deepening during the considered time span, which appears a reasonable assumption for the evolution of Alpine relief during the Quaternary (e.g., van der Beek and Bourbon, 2008).

We then calculate the flexural isostatic response to the inferred erosional unloading for a given lithospheric elastic thickness (T_e). For T_e = 10 km (Stewart and Watts, 1997), unloading produces maximum rock uplift of up to 1000 m in the Aosta-Valais area since 1.8 Ma (Figure 5). Due to the flexural response, rock uplift spreads out to the foreland of the belt, reaching 700 m in the Molasse Basin and 500 m in the Po plain. Differential rock uplift of ~200-300 m is observed in the Chambaran and Valensole areas, consistent with the elevation difference between the plateau surfaces and the modern river valleys. Modelled tilting in the Valensole area ranges between 0.25 and 0.30% to the SSW, whereas modelled tilting for the Chambaran Plateau is 0.25-0.5 % to the WNW. These results show that a significant part (~50%) of the inferred tilting of 0.5-0.8 % may be attributed to the isostatic response to increased Quaternary erosion in the Alps.

5. Discussion and conclusions

This study demonstrates that ~50% of the tilting recorded by Quaternary benchmarks in the Alpine foreland basin can be attributed to erosional unloading of the belt, in agreement with previous estimates (Champagnac *et al.*, 2007). However, whereas these authors compared their predictions to present-day uplift rates, the tilting observed here represents finite deformation over a long (*i.e.* entire Quaternary) time span. It is therefore insensitive to the effects of cyclic shorter-term processes such as glacial loading. We conclude that post-LGM glacial unloading and active glacier shrinkage account for at most half of the observed rock uplift. Similarly, a recent (post-LGM) increase in erosion rate (Hinderer, 2001) was invoked by Champagnac *et al.* (2007) to explain the discrepancy between rebound due to the average erosion over 1 Ma and more rapid present-day rock uplift in Switzerland. Here, however, we show that the total inferred erosion (including any increased post-LGM erosion), does not fully explain the integrated Quaternary tilting.

Some authors suggest tectonic mechanisms (e.g., active basal thrusting; Persaud and Pfiffner, 2004, Lardeaux *et al.*, 2006) to explain recent exhumation and active rock uplift of the western Alps. However, active crustal shortening and thickening should produce flexural isostatic subidence of the foreland (Burbank, 1992), in contrast with the observed rock uplift and erosion. Moreover, present-day shortening across the western Alps is null or negative (i.e. net extension; Calais *et al.*, 2002, Oldow *et al.*, 2002, Serpelloni *et al.*, 2005).

The other half of the observed tilting thus has to be explained by (an)other process(es), acting over a long time span (~2 Ma) and over an orogen-scale wavelength. These could include deep-seated geodynamic processes, such as mantle upwelling (Lyon-Caen and Molnar, 1989), slab break-off or delamination (Lippitsch *et al.*, 2003, Kuhlemann, 2007), or mineralogic changes (*e.g.*, de-eclogitisation of the lower crust; Kuhlemann *et al.*, 2002). Thus, even if the western Alps are considered to be in a “post-orogenic stage” (Delacou *et al.*, 2004, Selverstone, 2005, Sue *et al.*, 2007), the observed tectonic regime is a concequence of both external (climatic) and deep-seated controls that act on the belt to create significant deformation.

Acknowledgments

This work was supported by the Swiss National Science Foundation under the grants # PA002-117441, the INSU-CNRS “Reliefs de la Terre” programme and ETH Zürich (through S. Willett). We thank Paolo Frattini for sharing his alluvial fan data. JDC thanks Peter Molnar, Robert Anderson and Christian Sue for previous fruitful discussions. Guy Simpson and Jean Van Den Driessche provided insightful reviews.

References

Allen, P.A. and Hovius, N., 1998. Sediment supply from landslide-dominated catchments: implications for basin-margin fans *Bas. Res.*, **10**, 19-35, doi:10.1046/j.1365-2117.1998.00060.x.

Ballesio, M., 1972. Etude stratigraphique du Pliocène rhodanien *Doc. Lab. géol. Fac. Sci. Lyon*, **53**, 333 p.

Barletta, V.R., Ferrari, C., Diolaiuti, G., Carnielli, T., Sabadini, R. and Smiraglia, C., 2006. Glacier shrinkage and modeled uplift of the Alps *Geophys. Res. Lett.*, **33**, doi:10.1029/2006GL026490.

Blair, T.C. and McPherson, J.G., 1994. Alluvial fans and their natural distinction from rivers based on morphology, hydraulic processes, sedimentary processes and facies assemblages *J. Sed. Res.*, **A 64**, 450–489.

Bonnet, A. and Bornand, M., 1970. Pédologie et Quaternaire dans la vallée du Rhône moyen *Bull. Assoc. Fr. Et. Quat.*, 105-115.

Burbank, D.W., 1992. Causes of recent Himalayan uplift deduced from deposited patterns in the Ganges basin *Nature*, **357**, 680-683.

Burkhard, M. and Sommaruga, A., 1998. Evolution of the western Swiss Molasse basin: structural relations with the Alps and the Jura belt. In: *Cenozoic Foreland Basins of Western Europe* (A. Mascle, C. Puigdefàbregas, H.P. Luterbacher and M. Fernàndez, eds), pp. 279-298. Geological Society, London.

Calais, E., Nocquet, J.-M., Jouanne, F. and Tardy, M., 2002. Current strain regime in the Western Alps from continuous Global Positioning System measurements, 1996–2001 *Geology*, **30**, 651–654.

Cederbom, C., Sinclair, H., Schlunegger, F. and Rahn, M., 2004. Climate-induced rebound and exhumation of the European Alps *Geology*, **32**, 709-712.

Champagnac, J.D., Molnar, P., Anderson, R.S., Sue, C. and Delacou, B., 2007. Quaternary erosion-induced isostatic rebound in the western Alps *Geology*, **35**, 195-198.

Champagnac, J.D., Sue, C., Delacou, B., Tricart, P., Allanic, C. and Burkhard, M., 2006. Miocene lateral extrusion in the inner western Alps revealed by dynamic fault analysis *Tectonics*, **25**, doi:10.1029/2004TC001779.

Clauzon, G., 1990. Genèse et évolution du piémont néogène subalpin du Bas-Dauphiné. Université d'Aix-Marseille II, Aix-en-Provence.

Clauzon, G., 1996. Limites de séquences et évolution géodynamique *Géomorphologie*, 3-22.

Clauzon, G. and Rubino, J.-L., 1995. Peri-Mediterranean Pliocene basins are very large scale incised valleys filled by Gilbert-type fan deltas *Am. Assoc. Petrol. Geol. Bull.*, **79**, 1203-1204.

Crosta, G.B. and Frattini, P., 2004. Controls on modern alluvial fan processes in the central Alps, northern Italy *Earth Surf. Proc. Landf.*, **29**, 267-293.

Dade, W.B. and Verdeyen, M.E., 2007. Tectonic and climatic controls of alluvial-fan size and source-catchment relief *J. Geol. Soc.*, **164**, 353-358, 10.1144/0016-76492006-039.

Delacou, B., Sue, C., Champagnac, J.-D. and Burkhard, M., 2004. Present-day geodynamics in the bend of the western and central Alps as constrained by earthquake analysis *Geophys. J. Int.*, **158**, 753-774, doi:10.1111/j.1365-246X.2004.02320.x.

Demarcq, G., 1970. *Etude stratigraphique du Miocène rhodanien*. Editions BRGM, Paris.

Densmore, A.L., Allen, P.A. and Simpson, G., 2007. Development and response of a coupled catchment fan system under changing tectonic and climatic forcing *J. Geophys. Res.*, **112**, F01002, doi:10.1029/2006JF000474.

Dubar, M., 1984a. Chronologie et signification des dépôts continentaux du Néogène supérieur du bassin de Riez-Valensole *Bull. Soc. Géol. Fr.*, **26**, 971-978.

Dubar, M., 1984b. Les terrasses fluviatiles au Sud des Alpes *Bull. Assoc. Fr. Et. Quat.*, 134-138.

Dubar, M., Aguilar, J.-P., Chaline, J., Michaux, J. and Semah, F., 1998. Données chronologiques (mammifères et magnétostratigraphie) sur les dépôts plio-pleistocènes au toit du bassin de Valensole; implications morphodynamiques *Géol. France*, 57-68.

Dubar, M. and Semah, F., 1986. Paleomagnetic data bearing on the age of high terrace deposits (Durance sequence) in Alpine valleys of Southeastern France *Quat. Res.*, **25**, 387-391.

Fauquette, S., Suc, J.-P., Guiot, J., Diniz, F., Feddi, N., Zheng, Z., Bessais, E. and Drivaliari, A., 1999. Climate and biomes in the West Mediterranean area during the Pliocene *Palaeogeogr., Palaeoclim., Palaeoecol.*, **152**, 15-36.

Ford, M., Lickorish, W.H. and Kusznir, N.J., 1999. Tertiary foreland sedimentation in the Southern Subalpine Chains, SE France: a geodynamic appraisal *Bas. Res.*, **11**, 315-336, doi:10.1046/j.1365-2117.1999.00103.x.

Gigot, P., 1982. Carte Géologique de la France, Notice de la feuille de Forcalquier à 1:50.000. Bureau de Recherches Géologiques et Minières, Orléans.

Gudmundsson, G.H., 1994. An order-of-magnitude estimate of the current uplift rates in Switzerland caused by the Würm Alpine deglaciation *Eclog. geol. Helv.*, **87**, 545–557.

Guillaume, A. and Guillaume, S., 1982. L'érosion au Plio-Quaternaire dans les Alpes – Bilan quantitatif *Eclog. geol. Helv.*, **73**, 326–329.

Guzzetti, F., Marchetti, M. and Reichenbach, P., 1997. Large alluvial fans in the north-central Po Plain (Northern Italy) *Geomorphology*, **18**, 119-136.

Hay, W.W., Sloan II, J.L. and Wold, C.N., 1988. Mass/age distribution and composition of sediments on the ocean floor and the global rate of sediment subduction *J. Geophys. Res.*, **93**, 14993-14940.

Hinderer, M., 2001. Late Quaternary denudation of the Alps, valley and lake fillings and modern river loads *Geodin. Acta*, **14**, 231-263.

Hippolyte, J.-C. and Dumont, T., 2000. Identification of Quaternary thrusts, folds and faults in a low seismicity area: examples in the Southern Alps (France) *Terra Nova*, **12**, 156-162.

Hooke, R.L., 1968. Steady-state relationships on arid-region alluvial fans in closed basins *Am. J. Sci.*, **266**, 609–629.

Kahle, H.G., Geiger, A., Bürki, B., Gubler, E., Marti, U., Wirth, B., Rothacher, M., Gurtner, W., Beutler, G., Bauersima, I. and Pfiffner, O.A., 1997. Recent crustal movements, geoid and density distribution: contribution from integrated satellite and terrestrial measurements. In: *Results of the National Research Program 20 (NRP 20)* (O.A. Pfiffner, P. Lehner, P. Heitzmann, S. Müller and A. Steck, eds), pp. 251-259. Birkhäuser, Basel.

Kuhlemann, J., 2000. Post-collisional sediment budget of circum-alpine basins (central Europe) *Mem. Sci. Geol.*, **52**, 1-91.

Kuhlemann, J., 2007. Paleogeographic and paleotopographic evolution of the Swiss and Eastern Alps since the Oligocene *Global Planet. Change*, **58**, 224-236.

Kuhlemann, J., Frisch, W., Székely, B., Dunkl, I. and Kázmér, M., 2002. Post-collisional sediment budget history of the Alps: tectonic versus climatic control *Int. J. Earth Sci.*, **91**, 818-837.

Lardeaux, J.M., Schwartz, S., Tricart, P., Paul, A., Guillot, S., Bethoux, N. and Masson, F., 2006. A crustal-scale cross-section of the south-western Alps combining geophysical and geological imagery *Terra Nova*, **18**, 412-422, doi:10.1111/j.1365-3121.2006.00706.x.

Leeder, M.R., 1999. *Sedimentology and Sedimentary Basins: From Turbulence to Tectonics*. Blackwell, Oxford, U.K.

Lickorish, W.H. and Ford, M., 1998. Sequential restoration of the external Alpine Digne thrust system, SE France, constrained by kinematic data and synorogenic sediments. In: *Cenozoic Foreland Basins of Western Europe* (A. Mascle, C. Puigdefàbregas, H.P. Luterbacher and M. Fernàndez, eds), pp. 189-211. Geological Society, London.

Lippitsch, R., Kissling, E. and Ansorge, J., 2003. Upper mantle structure beneath the Alpine orogen from high-resolution teleseismic tomography *J. Geophys. Res.*, **108**, 2376, doi: 2310.1029/2002JB002016.

Lyon-Caen, H. and Molnar, P., 1989. Constraints on the deep structure and dynamic processes beneath the Alps and adjacent regions from an analysis of gravity anomalies *Geophys. J. Int.*, **99**, 19-32.

Mandier, P., 1988. *Le relief de la moyenne vallée du Rhône au Tertiaire et au Quaternaire. Essai de synthèse paléogéographique.* Bureau de Recherches Géologiques et Minières, Orléans.

Molnar, P., 2004. Late Cenozoic increase in accumulation rates of terrestrial sediment: How might climate change have affected erosion rates? *Ann. Rev. Earth Planet. Sci.*, **32**, 67-89.

Molnar, P. and England, P., 1990. Late Cenozoic uplift of mountain ranges and global climate change: chicken or egg? **346**, 29-34.

Mortaz-Djalili, D. and Perriaux, J., 1979. Le Néogène du Plateau de Chambaran (Bas-Dauphiné, France) *Géol. Alp.*, **55**, 133-152.

Oldow, J.S., Ferranti, L., Lewis, D.S., Campbell, J.K., Argenio, B., Catalano, R., Pappone, G., Carmignani, L., Conti, P. and Aiken, C.L.V., 2002. Active fragmentation of Adria, the north African promontory, central Mediterranean orogen *Geology*, **30**, 779-782.

Perriaux, J., Montjuvent, G. and Uselle, J.-P., 1984. Sédimentologie du Néogène du Bas-Dauphiné *Géol. France*, 105-114.

Persaud, M. and Pfiffner, O.A., 2004. Active deformation in the eastern Swiss Alps: post-glacial faults, seismicity and surface uplift *Tectonophysics*, **385**, 59-84.

Rubino, J.-L., Lesueur, J.-L., Guy, L. and Clauzon, G., 1990. *Le Miocène inférieur et moyen du bassin rhodanien. Stratigraphie séquentielle et sédimentologie*. Publ. Spéc. Assoc. Sédim. Fr.

Schlunegger, F. and Hinderer, M., 2001. Crustal uplift in the Alps: why the drainage pattern matters *Terra Nova*, **13**, 425-432.

Selverstone, J., 2005. Are the Alps collapsing? *Ann. Rev. Earth Plan. Sci.*, **33**, 113-132.

Serpelloni, E., Anzidei, M., Baldi, P., Casula, G. and Galvani, A., 2005. Crustal velocity and strain-rate fields in Italy and surrounding regions: new results from the analysis of permanent and non-permanent GPS networks *Geophys. J. Int.*, **161**, 861-880, doi:10.1111/j.1365-

246X.2005.02618.x.

Sileo, G., Giardina, F., Livio, F., Michetti, A.M., Mueller, K. and Vittori, E., 2007. Remarks on the Quaternary tectonics of the Insubria Region (Lombardia, NW Italy, and Ticino, SE Switzerland) *Boll. Soc. Geol. It.*, **126**, 411-425.

Small, E. and Anderson, R.S., 1998. Pleistocene relief production in Laramide mountain ranges, western Unites States *Geology*, **26**, 123-126.

Stewart, J. and Watts, A.B., 1997. Gravity anomalies and spatial variations of flexural rigidity at mountain ranges *J. Geophys. Res.*, **102**, 5327–5352.

Suc, J.-P. and Popescu, S.-M., 2005. Pollen records and climatic cycles in the North Mediterranean region since 2.7 Ma. In: *Early-Middle Pleistocene Transitions: The Land-Ocean Evidence* (M.J. Head and P.L. Gibbard, eds), pp. 147-158. Geological Society Special Publication, London.

Sue, C., Delacou, B., Champagnac, J.-D., Allanic, C., Tricart, P. and Burkhard, M., 2007. Extensional neotectonics around the bend of the Western/Central Alps: an overview *Int. J. Earth Sci.*, **96**, 1101-1129, 10.1007/s00531-007-0181-3.

Sue, C., Thouvenot, F., Fréchet, J. and Tricart, P., 1999. Widespread extension in the core of the western Alps revealed by earthquake analysis *J. Geophys. Res.*, **104**, 25611-25622.

van der Beek, P. and Bourbon, P., 2008. A quantification of the glacial imprint on relief development in the French Western Alps *Geomorphology*, **in press**.

Whipple, K.X., Kirby, E. and Brocklehurst, S.H., 1999. Geomorphic limits to climate-induced increases in topographic relief *Nature*, **401**, 39-43.

Zhang, P., Molnar, P. and Downs, W.R., 2001. Increased sedimentation rates and grain sizes 2-4 Myr ago due to the influence of climate change on erosion rates *Nature*, **410**, 891-897.

Figure Captions

Fig. 1: a) Simplified geological map of the western Alps. C and V indicate Chambaran and Valensole Plateau, respectively. A, Argentera; Aa, Aar; B, Belledonne; BPT, Basal Penninic Thrust; BR, Black forest; BZ, Briançonnais zone; DB, Dent Blanche nappe; DH, Dauphiné/Helvetic zone; DM, Dora Maira; GP, Gran Paradiso; L, Lepontine dome; M, Maure Massif; MoB, Molasse Bassin; MB, Mont Blanc; PZ, Piémont zone; P, Pelvoux; PN, Prealpine Nappes; URG, Upper Rhine Graben. b) Digital Elevation Model (DEM) of the western Alps showing the locations of the Figures 2 and 3 (black squares).

Fig. 2: a) DEM (*Institut Géographique National*, 50-m resolution) of the Chambaran Plateau, with points outlining Pleistocene abandonment surface digitized for the tilt calculations and 50 m isolines of rock uplift (see section 4 and Figure 5). White arrows indicate transport directions for Late Pliocene conglomerates making up the plateau surface (Mortaz-Djalili and Perriaux, 1979); inset shows rose diagram for transport directions and indicates both NE-SW (Rhone) and SE-NW (Isère) directed transport. b) Projection of plateau surface; the best-fitting plane has a slope of 0.93% (0.53°) in the direction N269 (r^2 = 0.954; RMS deviation = 35 m). A projection of the present-day long profile of the Isère River on the profile direction is shown for comparison.

Fig. 3: a) DEM of the Valensole Plateau, with points outlining southern parts of the surface used for tilt calculations and 50 m isolines of rock uplift (see section 4 and Figure 5), and projection direction of Figure 3c. b) Long profile of the Durance River and its terraces. The Matuyama-Brunhes transition (0.78 Ma) is recorded in the HT4 terrace level (Dubar and Semah, 1986). High Terraces (HT) are parallel to each other whereas lower terraces fan out toward the north,

possibly indicating a change in uplift/tilting in the mid-Pleistocene. c) Projection of the plateau surface; plateau remnants between the Asse and Colostre rivers are well fitted by a plane with a slope of 0.97% (0.56°) in the direction N224 (r^2 = 0.995; RMS deviation = 6.1 m). The upper part of the southernmost surface, between the Colostre and Verdon rivers, is characterized by a significantly higher slope close to the Digne thrust front, related to a local cone ("Breche de Balène") that was built onto the main surface (Dubar, 1984a). When not taking this upper part into account, the best-fit surface has a slope of 0.90% (0.52°) in the direction N233 (r^2 = 0.991; RMS deviation = 4.8 m). Projection of the present-day long profiles of the Bléône and Durance rivers onto the profile direction is shown for comparison.

Fig. 4: Scaling relationships between drainage area and fan area (top) and between drainage area and fan slope (bottom) for the Chambaran (open square) and Valensole (black circle) plateaux, compared to data from Guzetti *et al.* (1997; open triangles) and Crosta and Frattini (2004; crosses – only their data for non-eroding, non-obstructed fans have been used). Thick lines show best power-law fit to the combined data of Guzetti *et al.* (1997) and Crosta and Frattini (2004), dashed lines are 95% confidence limits. These fits are: $A_f = -0.93\ A_b^{(1.07 \pm 0.11)}$ (r^2 = 0.815) and $S_f = 1.04\ A_b^{(-0.51 \pm 0.05)}$ (r^2 = 0.807), where A_f is fan area (km^2), A_b is basin area (km^2), and S_f is fan slope (°). Quaternary tilt (vertical arrows) of surfaces is estimated as difference between present-day slope and predicted slope from power-law fit. Large fans in the Guzetti *et al*. (1997) dataset with slopes of 0.3-0.5° may have been influenced by active faulting (Sileo *et al*., 2007).

Fig. 5: Modelled rebound of the W-Alps in response to Quaternary erosion (calculated for T_e = 10 km and mass removal equivalent to basin fill over the last 1.8 Ma). Rebound is shown by 100-m contour lines; colour shading indicates tilting values. The Valensole (V) and Chambaran (C) areas are highlighted. A: Aosta; B: Briançon; D: Dignes; G: Geneva; Gr: Grenoble; L: Lyon; M: Marseille; N: Nice; S: Sion; T: Torino. See text for discussion of method.

Table 1. Plateau remnant characteristics, present-day and inferred initial slopes. The better fit of planes to the Valensole Plateau compared to the Chambaran reflects the better preservation of the surface in the former, as well as the fact that more detailed geological maps were available for digitization. Present-day combined upstream drainage area of the Rhone and Isère Rivers is taken for the Chambaran Plateau.

Plateau remnant	Area (km^2)	Best-fitting plane to present-day surface				Drainage area (km^2)	Inferred initial slope
		direction	slope	r^2	RMS (m)		
Chambaran	3000	N263E	0.93% (0.53°)	0.954	35	23450	0.07 – 0.18 %
Valensole C	400	N224E	0.97% (0.56°)	0.995	6.1	2600	0.25 – 0.49%
Valensole S		N233E	0.90% (0.52°)	0.991	4.8		

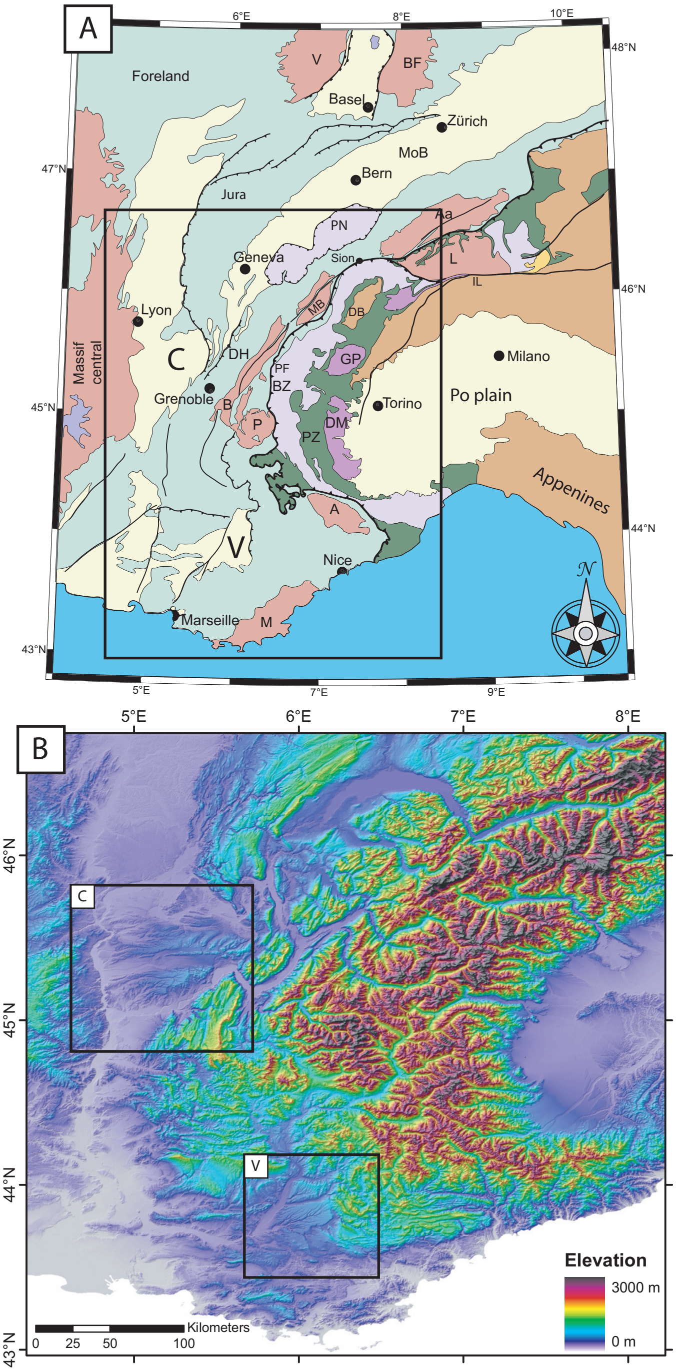

Fig. 1: a) geological map of the Western Alps. V and C for Valensole and Chambaran plateau, respectively b) DEM of the Alpine realm exhibiting the location of the Valensole and Chambaran plateaus (black squares).

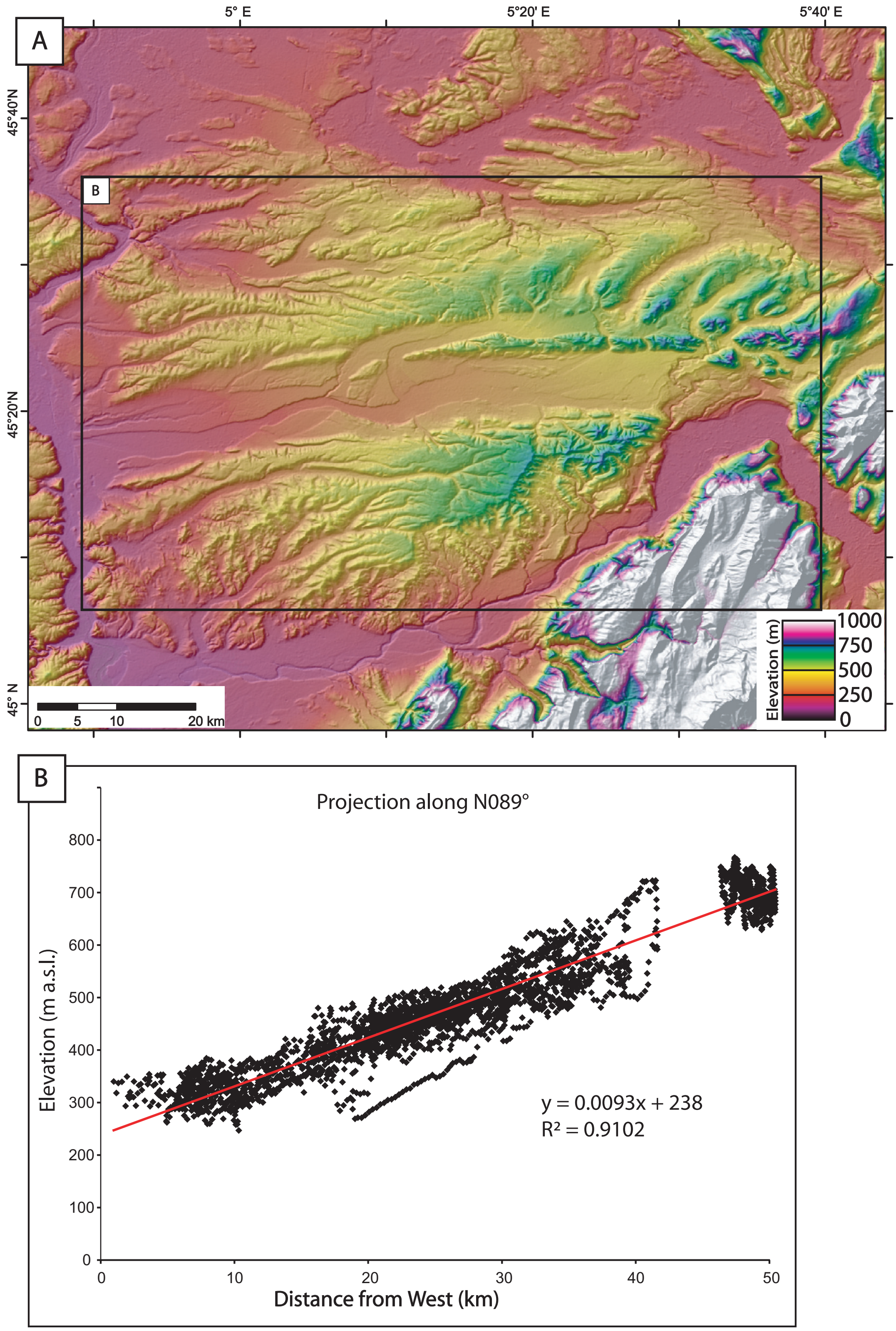

A
5° E
5°20' E
5°40' E
45°40'N
45°20'N
45° N
B
0 5 10 20 km
Elevation (m)
1000
750
500
250
0
B
Projection along N089°
Elevation (m a.s.l.)
Distance from West (km)
y = 0.0093x + 238
R² = 0.9102

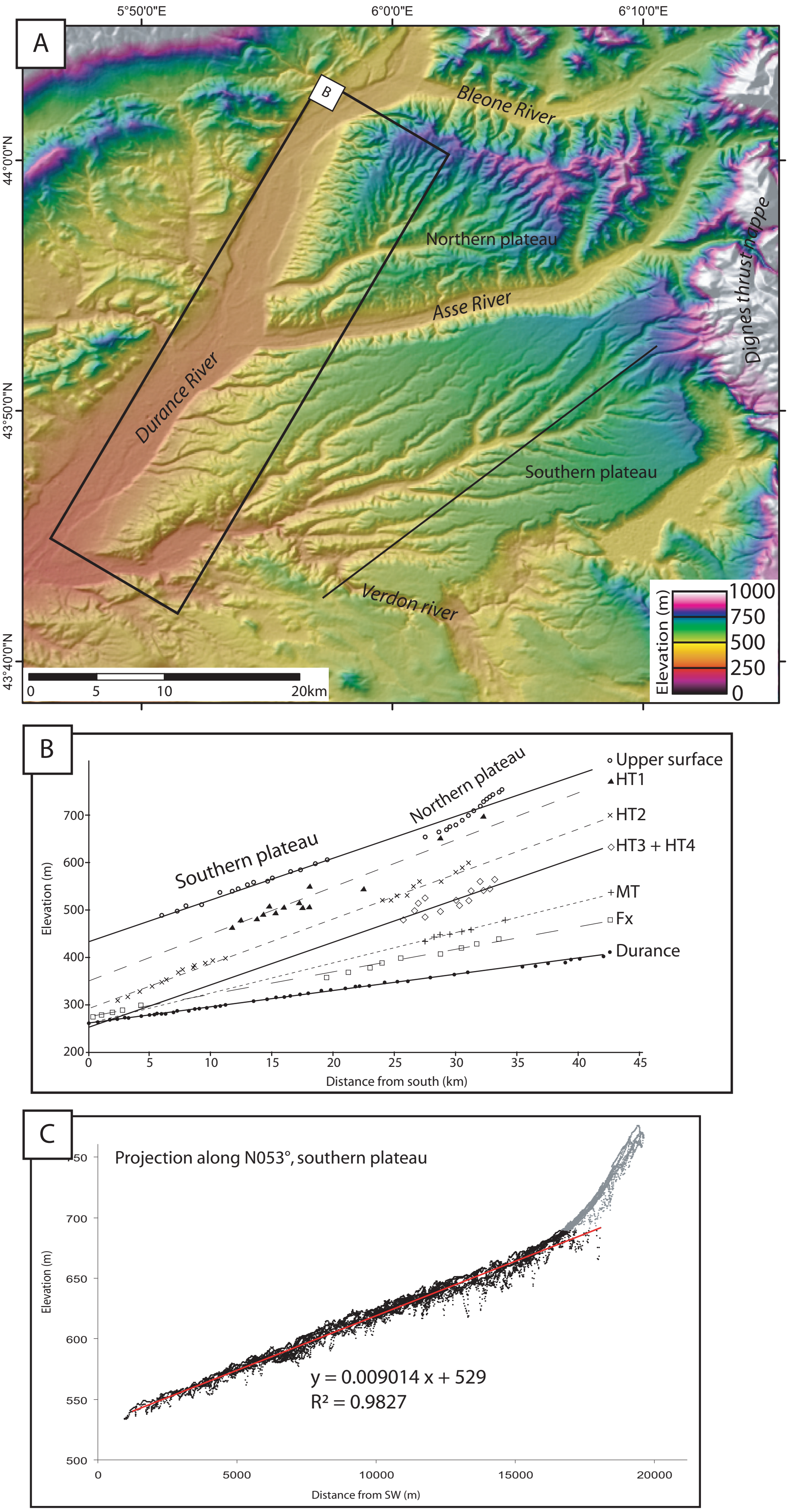

Fig. 3: a) DEM of the Valensole plateau area, b) cross section of the quaternary terraces of the Durance River. Note the parallel upper surface, HT1, HT2 and HT3+HT4, and the fan-like disposition of the younger terraces. Note also the short vawelengh deformation of the northern plateau. c) Projection along the N053 direction of the preserved villafranchian surface of the southern plateau. Note that the gray dots belong to the more recent "Breche de Balene" proximal fan, thus are not considered in our slope determination. The slope of the best fit line is 0.09%.

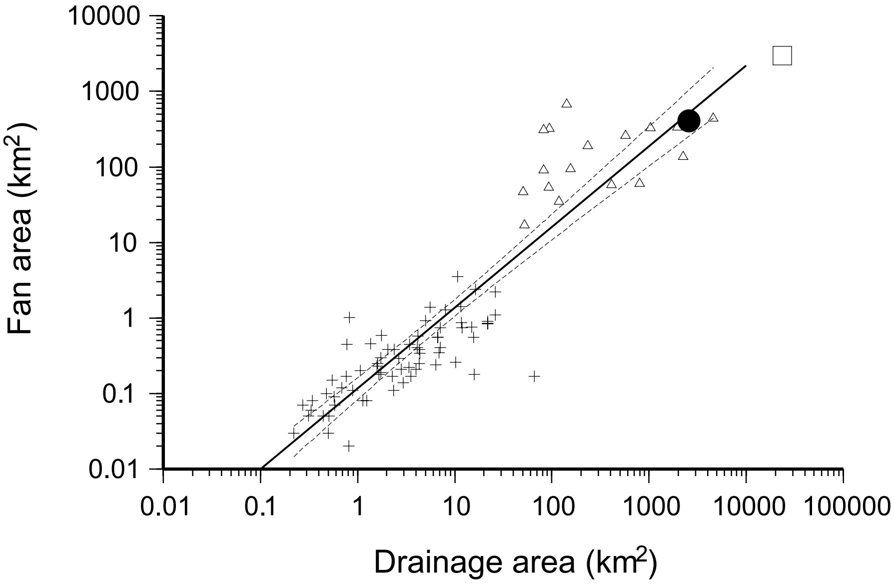
10000
1000
100
10
1
0.1
0.01
Fan area (km2)
0.01
0.1
1
10
100
1000
10000
100000
Drainage area (km2)

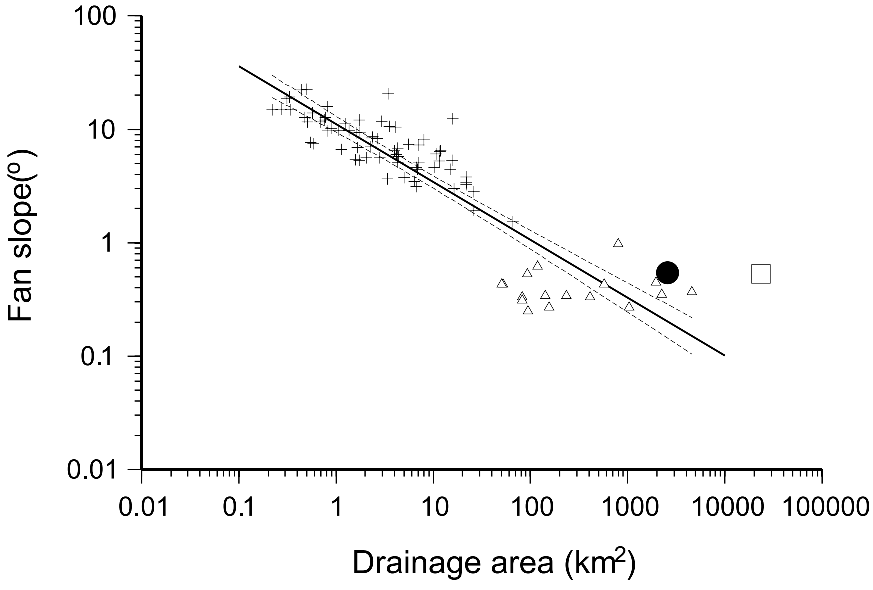
100
10
1
0.1
0.01
Fan slope(o)
0.01
0.1
1
10
100
1000
10000
100000
Drainage area (km2)

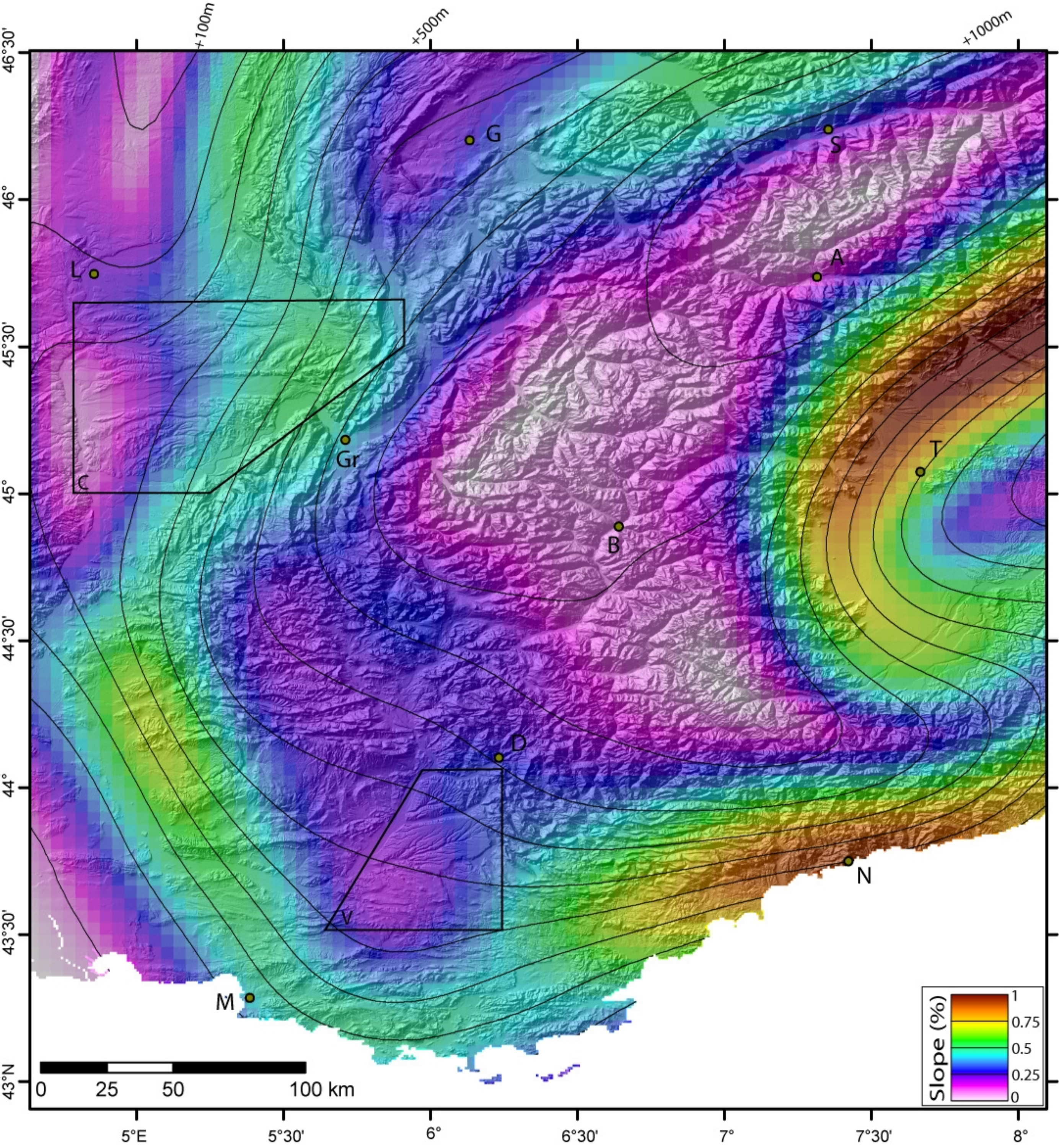

Fig. 5: Model of the Quaternary rebound of the W-Alps for the last 2Ma (+100m contour lines) and associated tilting of a hypothetic surface over the Alps. Valensole (V) and Chambaran (C) area are highlighted. Te=10km. G: Geneva; S: Sion; A: Aosta; L: Lyon; Gr: Grenoble; B:Briançon; T: Torino; D: Dignes; N: Nice; M: Marseille.